

SUPPLEMENTARY METHODS

1. Genetic mapping and sequencing of the *pma* candidate region

The *pma* mutation was genetically mapped using microsatellites across the previously identified candidate region. Homozygote *pma/pma* founder males were bred with BALB/c females and the [PMA x BALB/c] F1s were backcrossed with *pma/pma* homozygotes. 871 backcross [BALB/c x PMA] F1 x PMA pups were obtained and scored as clubfoot or normal at birth, of which 616 were normal and 255 had clubfoot. This deviated from expected 50:50 ration and is consistent with incomplete penetrance of the phenotype on a mixed genetic background, as described previously (Kato et al., 1995). Because the genotype of 'normal' pups could not therefore be determined with certainty, 199 clubfoot mice (inferred to be certainly *pma/pma*) were successfully genotyped with a panel of microsatellites (D5Mit 218, D5Mit166, D5Mit 282, D5Mit 219, D5Mit60, D5Mit33, D5Mit32 and D5Mit9 – see Table 1 (main text) and Supplementary Table S1 below) to identify regions of genomic homozygosity associated with the clubfoot phenotype. Two BALB/c founders, two PMA founders (*pma/pma*), 2 [BALB/c x PMA] F1 and 3 'normal' (presumed *pma/+*) [BALB/c x PMA] F1 x PMA backcrosses were also analysed as controls.

There were 12 potentially informative crossovers identified, which located the mutation to 2.5 Mb bounded by D5Mit166 (Chr5:133146598-133146706 bp) and D5Mit60 (Chr5:135715435-135715564 bp) (Figure 6). This reduced candidate region still contained 39 genes. To further define the candidate region, targeted next-generation resequencing was performed on two recombinant mice (one with crossover distal to the mutation, and one proximal to the mutation), three parental *pma/pma* and three parental BALB/c mice. 3.04 Mb encompassing the entire candidate region between D5Mit166 and D5Mit60 was obtained from all mice. Nearly 9000 polymorphic SNPs and indels within this region were interrogated to determine the minimum candidate region within which backcross mice were homozygous for PMA founder alleles. This analysis defined crossovers at approximate positions Chr5: 134514245 and Chr5: 134483438, defining a 0.89 Mb candidate region containing 13 genes: *Gatsl2*; *Wbscr16*; *Gtf2ird2*; *Ncf1*; *Gtf2i*; *Gtf2ird1*; *Cyln2 (Clip2)*; *Lat2*; *Gm52*; *Rfc2*; *Eif4h*; *Limk1* and *Eln*. Within this 0.89 Mb candidate region, nearly 4075 SNPs and small insertions or deletions (indels) were identified that were unambiguously homozygous for the *pma* allele in all clubfoot crossover animals and not found in BALB/c. Restricting the analysis only to the annotated genes in the region yielded 2053 SNPs and indels, of which 470 were novel mutations that had not previously been identified in any other

mouse line. Any of these could represent the pma mutation and represented too many to analyse indiscriminately. The dataset was therefore filtered to remove any mutation that did not potentially affect the processed mRNA or protein – i.e. intronic sequence and intergenic sequence was removed, and all synonymous coding polymorphisms, though it was recognised that any of these SNPs and indels may still be pathogenic. The refined list contained 23 SNPs that were predicted to cause either nonsynonymous changes in amino acid sequence of the gene product (5 SNPs – Table 2) or changes in the untranslated region of the processed mRNA (18 SNPs, all located in 3' UTR) (Supplementary Table S2). The analysis of these candidates is described in the main text.

2. **Motor neuron explant collagen-cultures.**

Collagen gel was prepared by mixing 180 ml bovine collagen (6 mg/ml) with 180 ml rat collagen solution, 40 ml 10x DMEM culture medium and 20 ml 0.8 M sodium bicarbonate. Gel was kept on ice. 40 ml of collagen gel was dispensed into each well of a 4-well plate. A pipette tip was used to ensure the gel covered the whole of the well surface. Plates were incubated for 45 minutes at 37°C.

Neural tube was dissected out of sagittally bisected embryos. Neural tube was rotated such that the ventral-most portion faced up, then the neural tube was cut longitudinally to separate the ventrally located motor column from the rest of the spinal cord. The motor column was added to cold culture medium and kept on ice.

Each complete motor column was cut into three equal portions immediately prior to transferring them into the culture dish. 800 µL of culture medium was added to the centre of each well after the gel had set. The dissected and divided motor column portions were to each well using the 200µL pipette. The portions were in very close proximity to one another. If the portions are too large they settle poorly and if they are too far apart, few axons project. Samples were cultured for 72 hrs at 37°C without moving the plate.

Supplementary Table S1: Full genomic analysis

[Click here to Download Table S1](#)

Supplementary Table S2: Filtered mutations

[Click here to Download Table S2](#)

Supplementary Table S3: phenotype of pma x EPHA4 compound hets and controls

[Click here to Download Table S3](#)

Supplementary Table S4: Pan-genomic microsatellite allele screen

[Click here to Download Table S4](#)

Supplementary Table S5: Microsatellite primers and fragment lengths

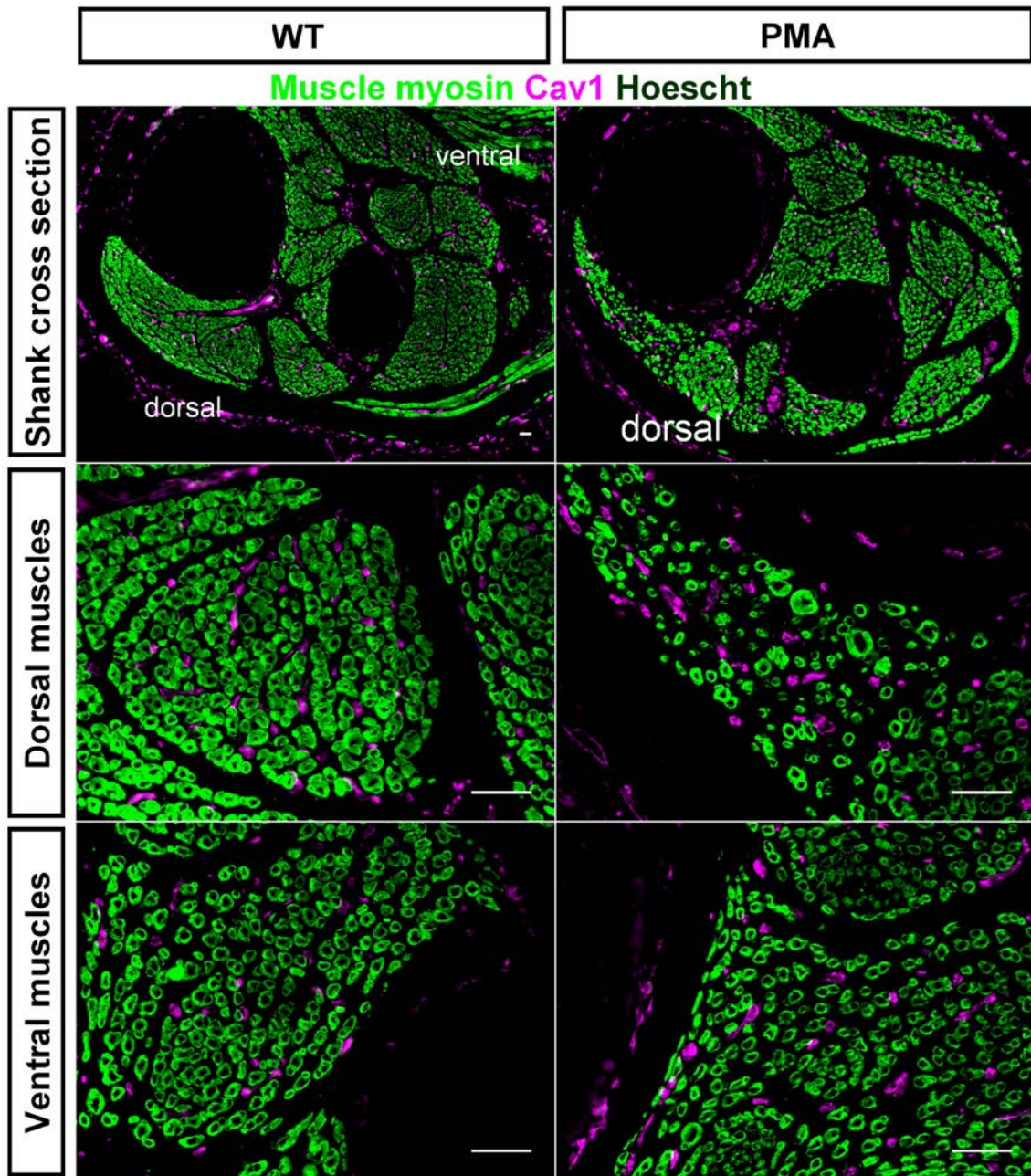
Primers used for microsatellite fragment length analysis

	Position (Chr5)	Primer name	Labelling	Sequence	Fragment size (bp)	
					BALB/c	PMA
D5Mit218	132937774-132937901	D5Mit218_F	6FAM	ACATTTATCATTGCTTCTGTTTCATG	128	91
		D5Mit218_R		CTGCATTAATACACACAAACATATGC		
D5Mit166	133146598-133146706	D5Mit166_F	VIC	GTGTAAGTGCAGTTTCTCTGTCTG	109	112
		D5Mit166_R		TCTTCAATTGAGAGTATCTTGTCCAGG		
D5Mit428	134150428-134150551	D5Mit428_F	NED	CCTCATGATTTGCTTGGCTT	125	125
		D5Mit428_R		CCATACCTGGGCTGGAGTC		
D5Mit282	135222563-135222664	D5Mit282_F	PET	GTCTTTGCTTGGAGATGTTCCG	105	109 (106)
		D5Mit282_R		AACATAGTATGAAACACACACGGG		
D5Mit219	135316925-135317048	D5Mit219_F	6FAM	TGCCTTGTTTCCTATCCACC	122	133 (131)
		D5Mit219_R		GACTATATAGTGAGATCCGGGCC		
D5Mit60	135715435-135715564	D5Mit60_F	VIC	AACCGCATCCATTCCTAGC	132/134	127
		D5Mit60_R		TAAGCACCAAGGAAACCAGG		
D5Mit33	135829291-135829405	D5Mit33_F	NED	ACTCACAACCTTTCTGTCTTAGCC	111	86
		D5Mit33_R		AAACATAATTAGCTGGGCATGG		
D5Mit32	135920110-135920232	D5Mit32_F	PET	TCACTGAGAGATGTGCAGGG	124	137
		D5Mit32_R		AAACTGACCCAGGACTCCG		
D5Mit97	137003596-137003722	D5Mit97_F	6FAM	CAATACAAACGGCAAGACCC	118	124
		D5Mit97_R		CACACAAGTAACTTTAGACGGGG		

Supplementary Table S6: gPCR primer sequences for 20 genes spanning the candidate region.

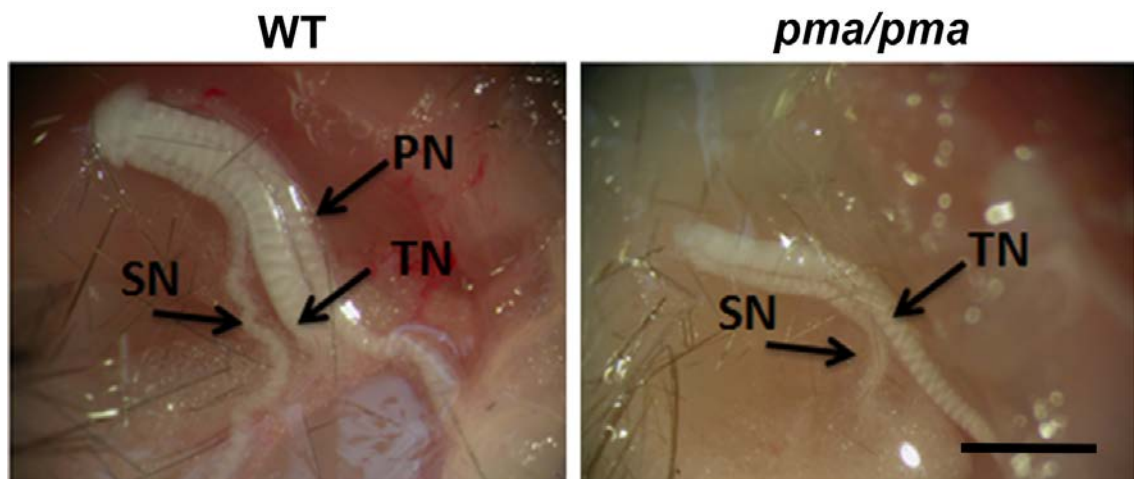
Primer name	Forward 5'-3'	Reverse 5'-3'
<i>Auts2</i>	GATGACACTGGTAGACTTGC	CTACAGTGCATGAGACCATG
<i>Ras A4</i>	GTTGGCAAACCTAGGCCTAAG	GGCAAGTGTACTTGGTAGTC
<i>Dtx2</i>	TGTGAAACACTAGGAGCTGAG	CAGATTCAACTCCTAGCACC
<i>LimK1</i>	CCCTGATGTGACTCATTTGC	GGTTCATTAGGCTTAGCAGC
<i>Serpine1</i>	CAGTAAGAACAACAGGAGCTG	GGCTGACCTTGAATTCATGG
<i>Fzd9</i>	GGCATTGGCTACAACCTGAC	CTCCACGTAAGTGAACCTCTC
<i>Ncf1</i>	CACACAGAGATCTATCTGCC	CCTTCTGCAGATACATGGATG
<i>EphB4</i>	GCTCAGAGGATAAAGAGGAC	GTCACAATGCAGATGGTCAG
<i>Hip1</i>	CTAGCATGCACAAAGTTCCG	GTCTCACCCAATACAAAGCG
<i>Gtf2i</i>	CAGTAAGTAAACCAGGAGGC	CAAGAAGAGCTCCAGCTTAC
<i>Trim50</i>	CCGGCTACTGCCACCCTCT	GACCCCAAGCGCCAGTCAC
<i>Por</i>	CTTGGCCGACCTGAGCAGCC	AGTCCTGCGGTTGTCTGGTG
<i>Gats</i>	TTGCCAGCGTCGCCAAGGAG	GGCCAGCCAGGTGGCATCAG
<i>Stx1A</i>	CCATGAGGCTCCCGTCCCA	CGAGTCTTGCCCCGCACTGG
<i>Eln</i>	GGCATGTCTAATCCCGTGCAT	GCGTGCATGCGTGCAATAGCG
<i>Rik</i>	GCTCAAATCGTCGAGGACC	GTGCATGCCGTAAGTCGTGC
<i>Ywhag</i>	CTTGGTGAGTCAGCACTGTC	CGTCATGTCATGTACCATGCAC
<i>cut1</i>	GGCGCCTGACTATACGTG	GGTCAGTCAGTCAGTCTGTAC
<i>fis1</i>	TGCAGCTGCATGCAACGTC	GACTGCCCTGCATGCATGCTAG
<i>Rhbdd2</i>	GTAAGTGCACGTGCATAAAGC	GTACGTGCGGTACGGGTAGGC

FIGURE S1: Vascularisation of muscles in the PMA mouse



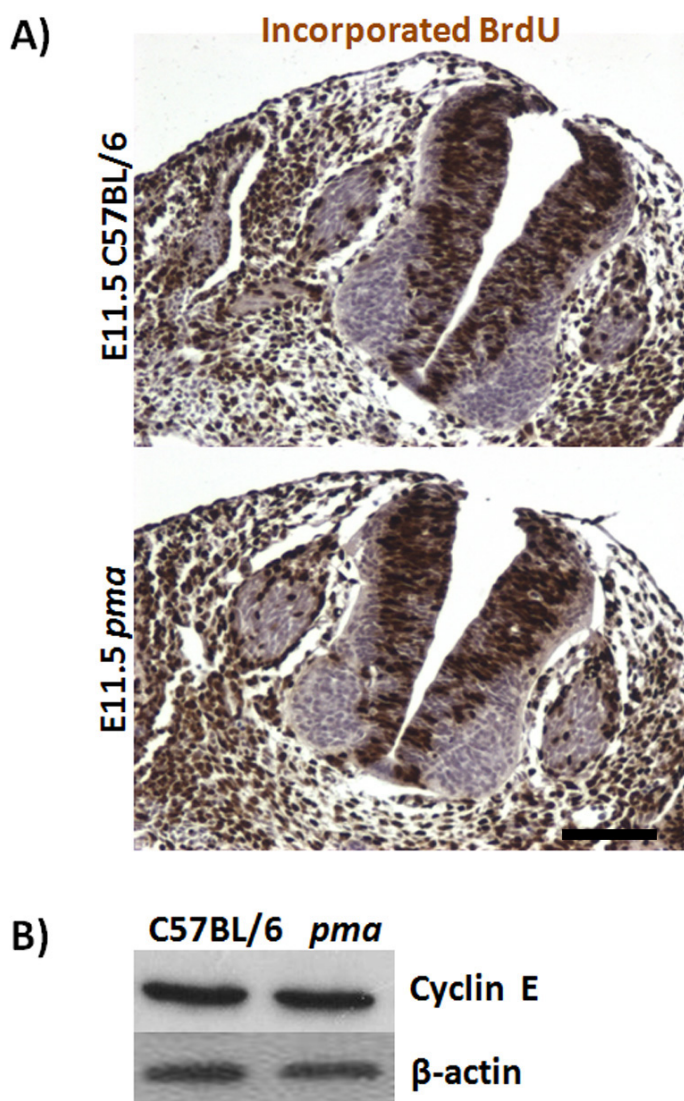
Legend: Immunohistochemistry for blood vessel marker, Caveolin (magenta) and muscle marker, myosin (green) in cross sections of the calf of E16.5 wild-type (left) and *pma/pma* homozygous mice (right). Dorsal and ventral muscles are shown at higher magnification. In contrast to failure of dorsal innervation in *pma/pma* homozygotes (Main text: Figure 1), dorsal muscles are fully vascularised. Scale bar represents 50 μ m.

Figure S2: Absence of peroneal nerve in *pma/pma* homozygotes

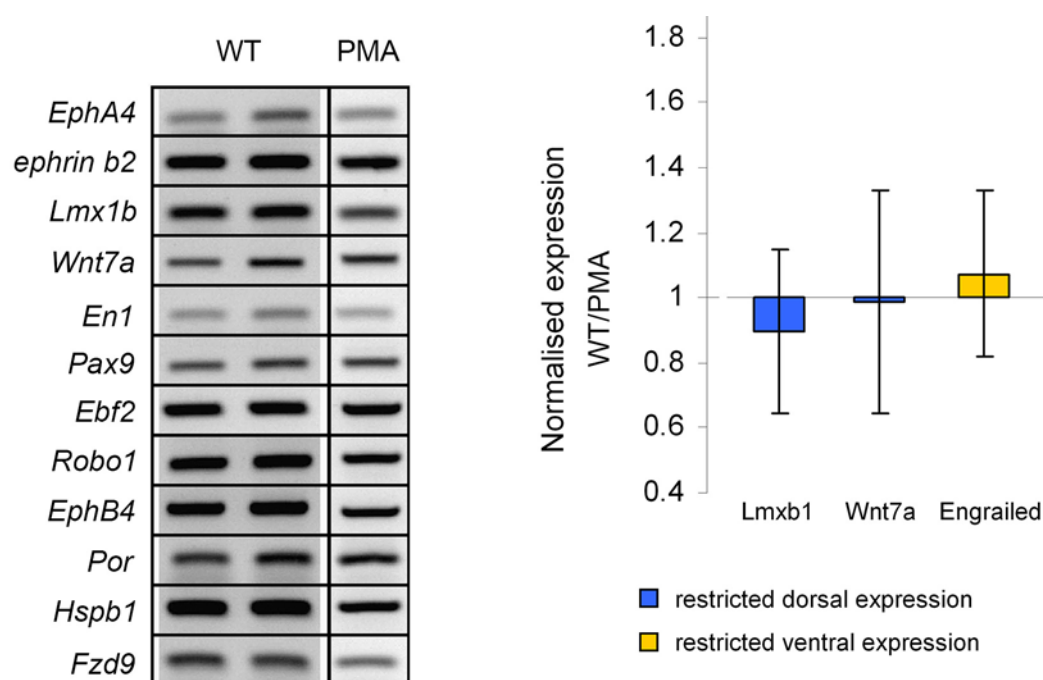


Legend: Dissections of wild-type (left) and *pma/pma* neonates exposing branches of the sciatic nerve in the hindlimb. The peroneal nerve (PN) is absent in the mutant. Abbreviations: PN, peroneal nerve; TN, tibial nerve; SN, sural nerve. Scale bar represents 4 mm.

Figure S3: Proliferation and cell death in neural tube development in the *pma* embryo

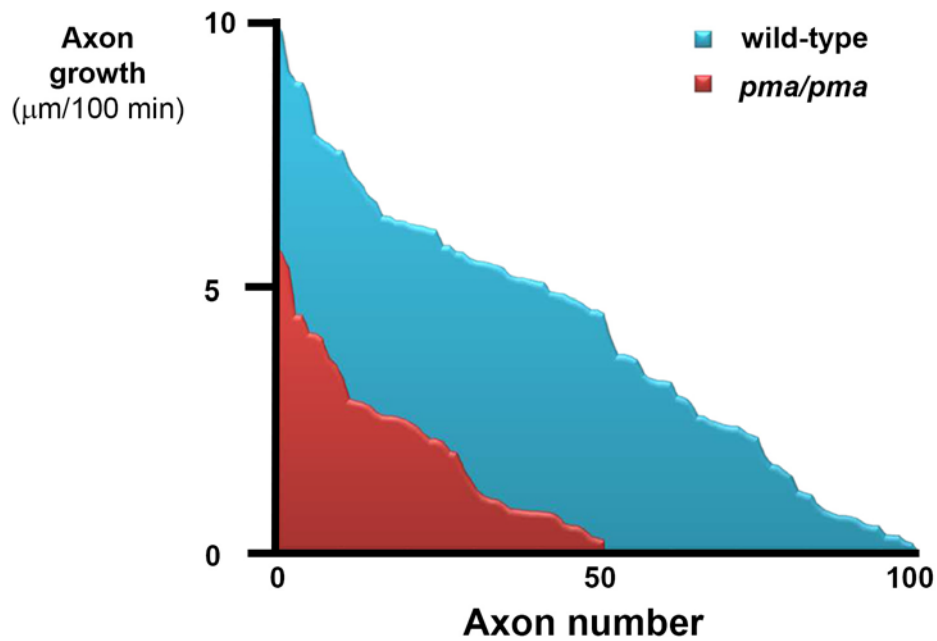


Legend: (A) Incorporation of BrdU (brown) by proliferating neurons in the developing neural tube shows no difference in cell proliferation at E11.5 between the *pma/pma* and wild-type embryos. The sections were counterstained with haematoxylin. The data were not quantified but it was clear there was no gross failure of proliferation in the ventral neural tube of *pma/pma* embryos. (B) Mitotic protein Cyclin E was assessed by western blot, but no changes were found between the *pma* and C57BL/6 embryos. β -Actin is shown as a loading control. Scale bar represents 60 μ m.

Figure S4 – Expression of developmental genes in *pma*-mutant hindlimb mesenchyme.

Legend: RT-PCR data using cDNA synthesised from E11.5 hindlimbs of wild-type and *pma/pma* embryos. Left – semi-quantitative PCR bands for genes that are known to be expressed in the hindlimb in a dorso-ventral restricted pattern (*EphA4*-*Ebf2*) and genes on chromosome 5 in the *pma* region defined by Katoh et al. (1995) (*EphB4* – *Fzd9*). No obvious difference between wild-type and *pma* mutants. Right – qPCR of normalised gene expression (from three replicates) for dorsal mesenchyme genes, *Lmx1b* and *Wnt7a*, and ventral mesenchyme gene, *En1*. There are no significant differences between genotypes.

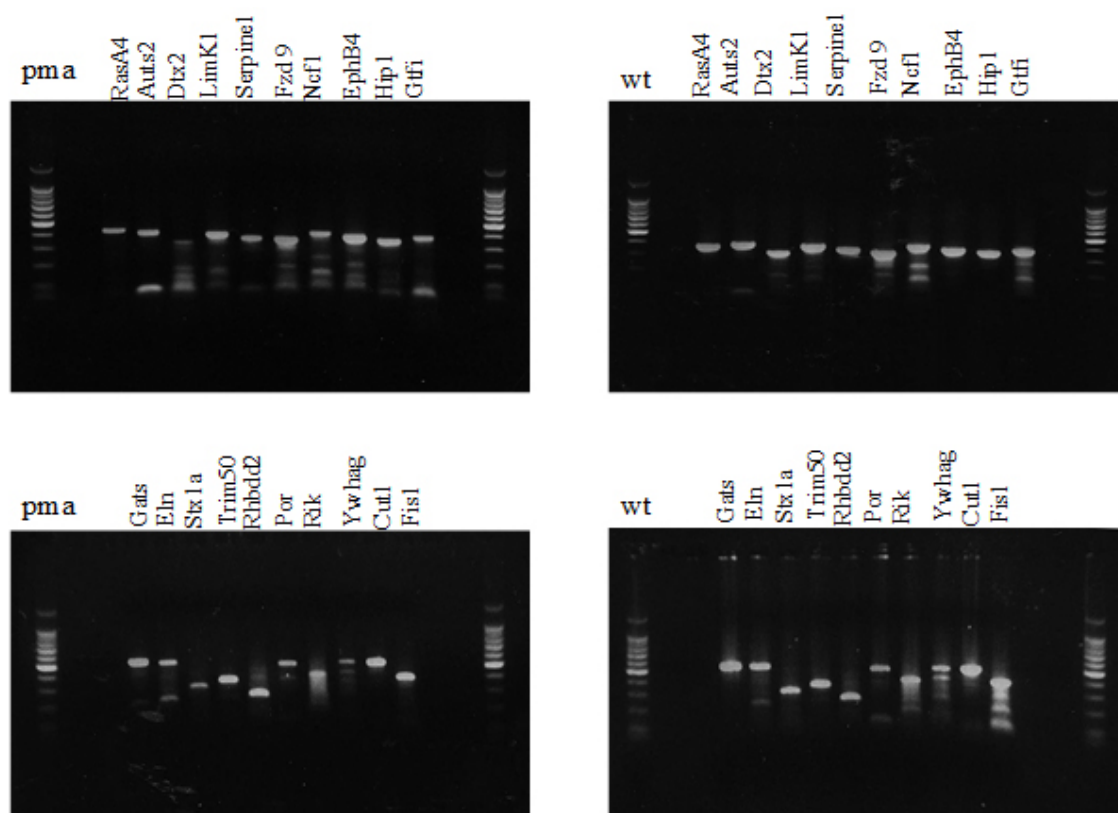
Figure S5. Growth cone extension of wild-type and *pma/pma* neurones in culture



Legend: Growth rate measured in vitro for 97 wild-type and 50 *pma/pma* lateral motor column (LMC) motor neurones, arranged in order from fastest to slowest. There was very considerable variation in both genotypes, but the distributions were similar, suggesting a general reduction in growth cone extension in *pma* mutants, independent of their original lateral or medial specification within the LMC.

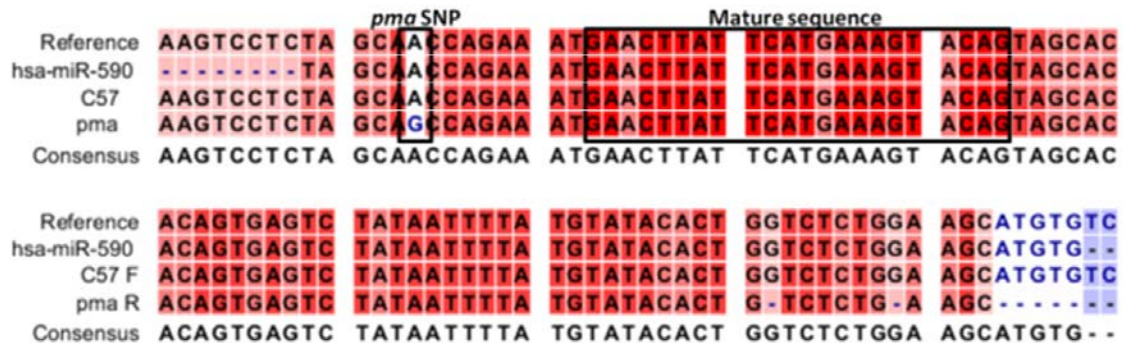
Figure S6

Genomic PCR for 20 genes across the initial 4.8 Mb candidate region for pma.



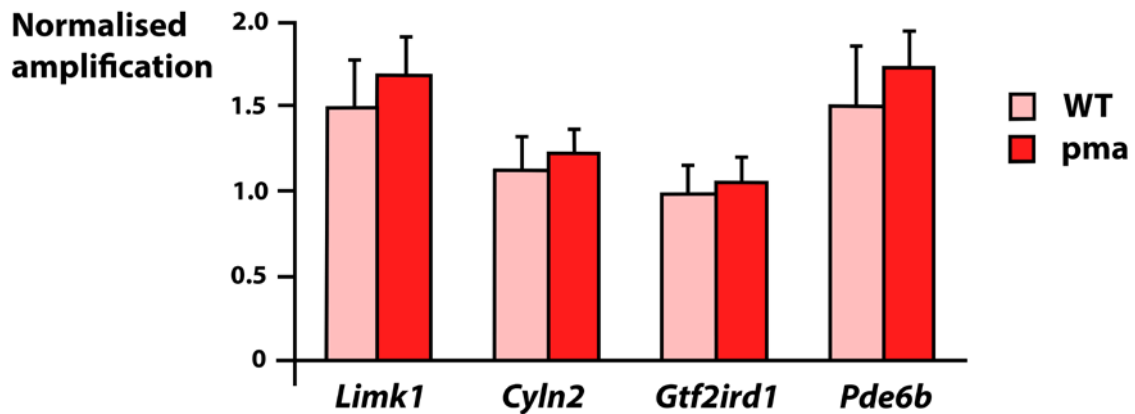
Bands were expected at the following molecular weights: RasA4: 531bp, AutS2: 516bp, Dtx2: 286bp, LimK1: 337bp, Serpine1: 229bp, Fzd9: 474bp, Ncf1: 378bp, EphB4:446bp, Hip1: 508bp, Gtfi: 377bp, Gals: 386bp, Eln: 389bp, Stx1a: 325bp, Trim50: 377bp, Rhbdd2: 347bp, Por: 322bp, Rik: 394bp, Ywhag: 395bp, Cut1: 348bp and Fis1:380bp. The marker is a 100 bp ladder, with the bright band representing 500 bp. All genes were present and all bands were the expected size in pma, suggesting no gross deletions in the region in the mutant mice. PCR primers are listed in Supplementary Table S6.

Figure S7 Micro RNA mmu-miR590-5p



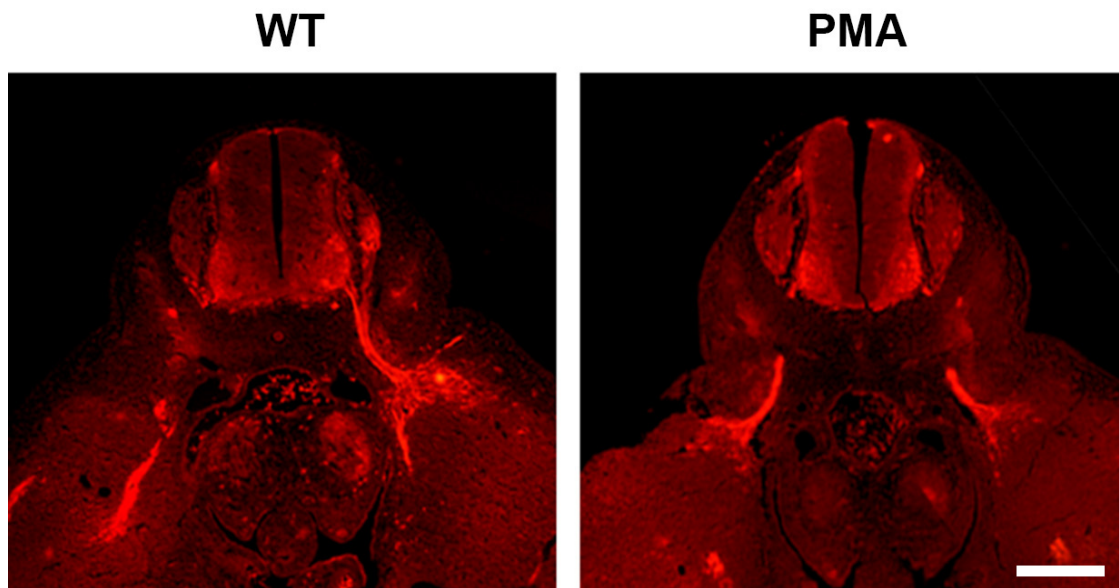
Legend: The sequence of mmu-miR590 in *pma* mice was investigated by amplifying the core and flanking regions through genomic PCR and compared with both reference BALB/c and C57BL/6 sequence. Sequence of mmu-miR590-5p in *pma* homozygotes. Reference sequence at top. Has-miR-590 = human sequence. C57 = C57BL/6 sequenced as control. *pma* = sequence from *pma/pma* homozygotes. There is a A/A to G/G substitution in PMA animals but this affects a peripheral pre-miRNA nucleotide, predicted not to affect the functional mature sequence which is unchanged.

Figure S8: Copy number analysis of candidate region.



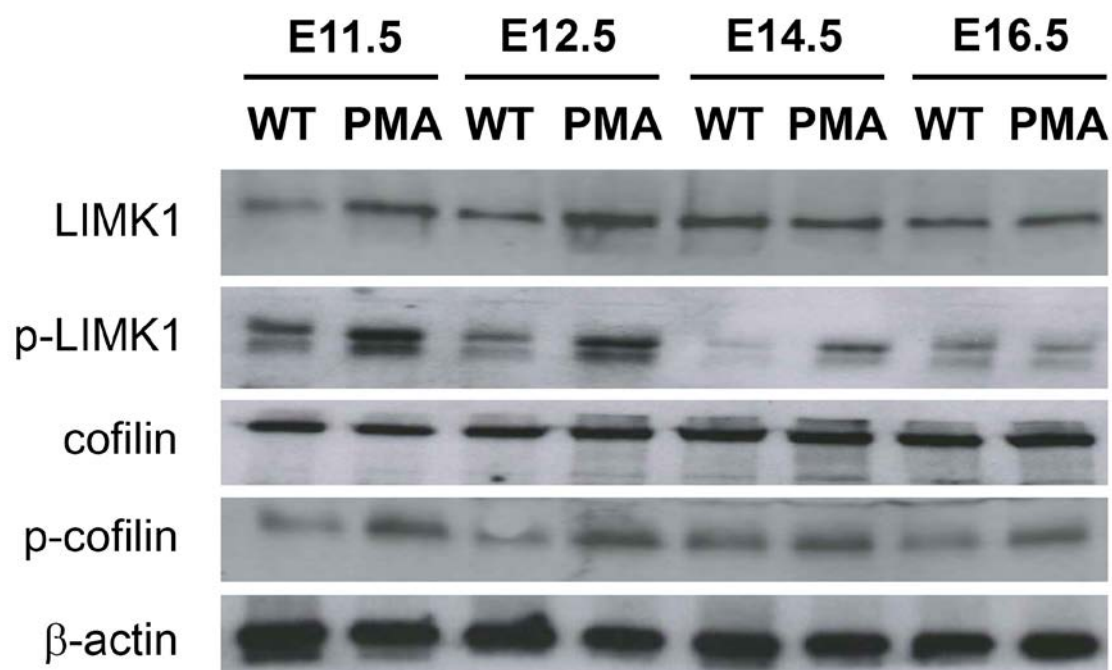
Copy number results based on qPCR of genomic DNA from livers of WT mice and *pma/pma* homozygotes, normalised against reference gene RNaseP. All data are mean \pm SEM based on 4 independent replicates. Genes were selected based on position at the proximal (*Gtf2ird1*), central (*Cyln2*) or distal (*Limk1*) part of the candidate region, or linked but 20 Mb outside the candidate region (*Pde6b*). Efficiency of amplification varied between primer sets, but there was no significant difference between wt and *pma/pma* samples at any locus.

Figure S9: Cyln2 (CLIP2) localisation to developing sciatic nerve motor neurons.



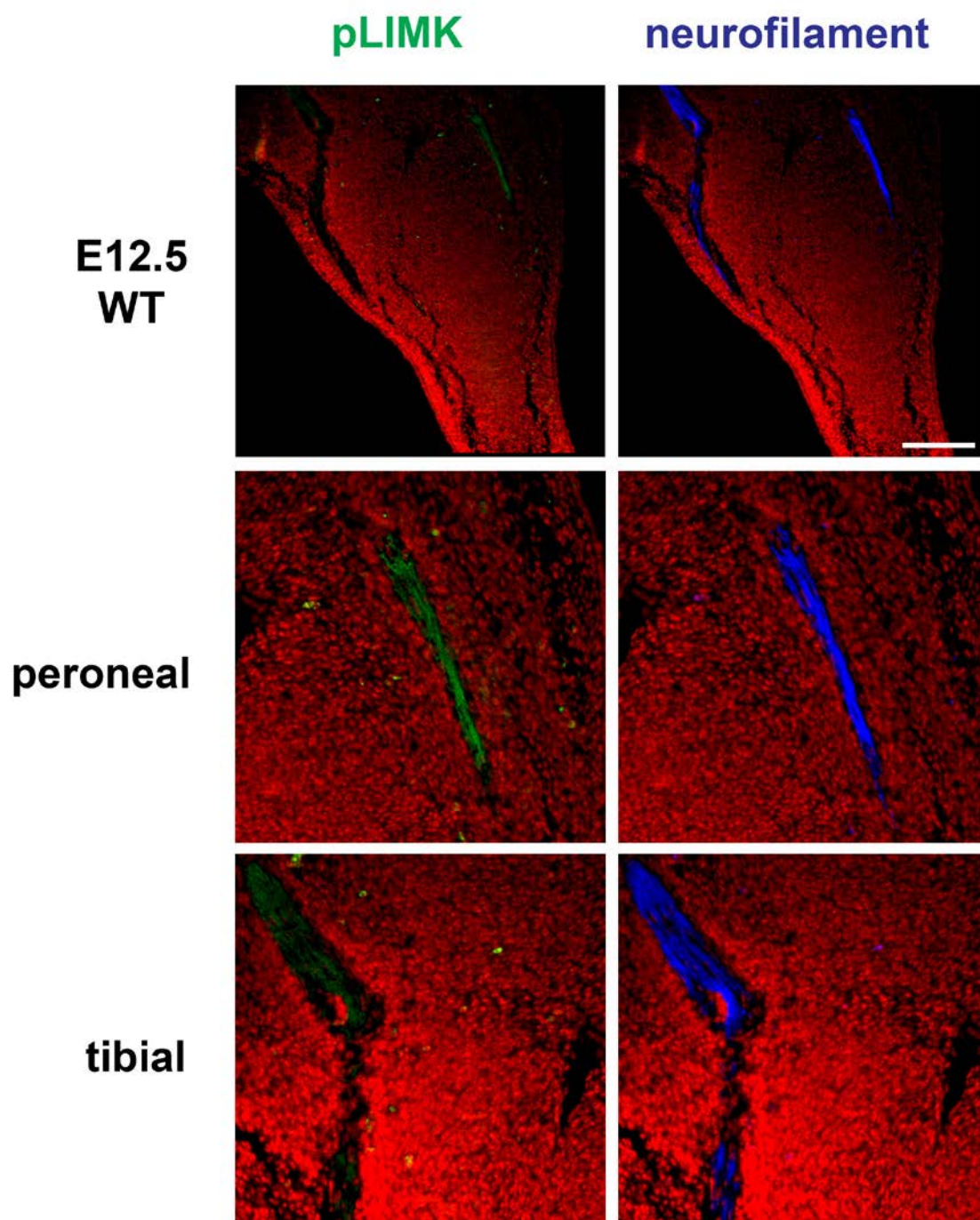
Legend: Fluorescence immunohistochemistry for Cyln2 localisation (red) in E12.5 wild-type (left) and *pma/pma* (right) embryos. Cyln2 is strongly detected in the lateral motor columns and projecting axons of embryos of both genotypes. Scale bar represents 100 μm .

Figure S10: Western blot analysis of PMA embryos at E11.5-E16.5.



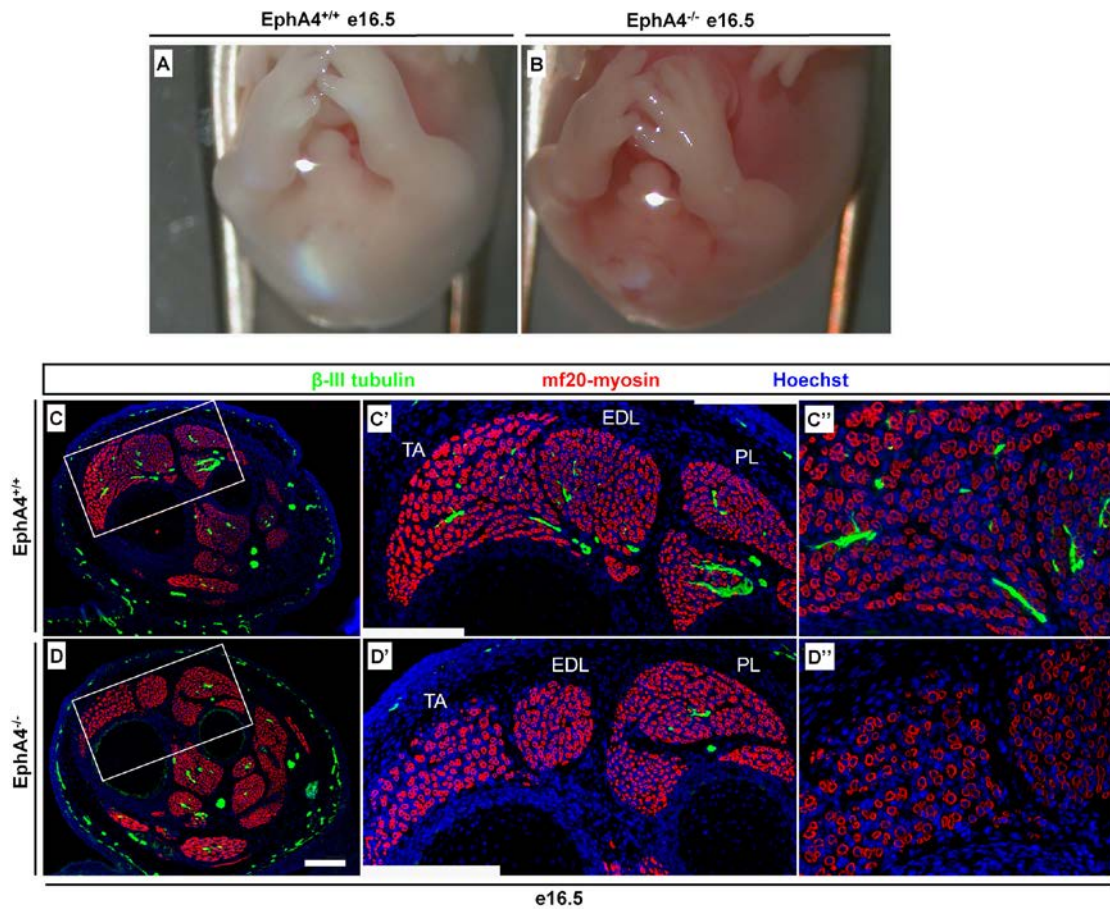
Legend: Western blots (representative of at least 3 replicates) comparing wild-type (WT) with *pma/pma* (PMA) embryos at E11.5 to E16.5. Total LIMK1 and phosphorylated LIMK1 are quantitatively increased in PMA homozygotes at E11.5 and E12.5, with higher levels of phosphorylated LIMK1 still identifiable at E14.5. Total cofilin levels (a target of LIMK1 kinase activity) are unaffected by genotype, but levels of phosphorylated cofilin increased, consistent with increase in LIMK1 activity. β-actin used as loading control. It is not clear why p-LIMK1 produced a doublet band in this blot, although it may be a result of proteolysis in this particular preparation.

Figure S11: p-LIMK localisation in dorsal and ventral branches of the wild-type sciatic nerve.



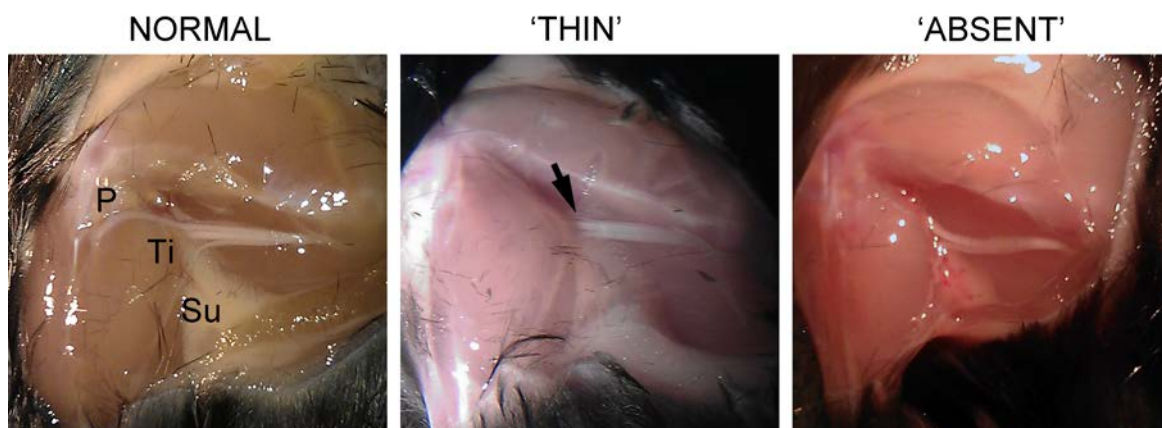
Legend: Immunohistochemical analysis of p-LIMK1 in E12.5 wild-type limb bud. Top row. Double labelling for p-LIMK1 (green), neurofilament (to label all nerves) (blue). Peroneal branch of the sciatic nerve is at right, tibial branch on right. Bottom two rows are detail of top row, showing peroneal and tibial branches separately. P-LIMK1 levels are higher in peroneal than in tibial nerves. Scale bar represents 400 μ m.

Figure S12: Innervation of hindlimbs of EphA4-null mice



Legend: (A, B) Hindlimbs of E16.5 wild-type (A) and *EphA4*^{-/-} (B) littermates, showing the limb position prior to foot rotation which fails in the mutants. At this developmental stage, the wild-type and mutant foetuses have outwardly indistinguishable limb morphologies. (C, D) immunohistochemistry on tissue sections through the lower hindlimbs of wild-type (C-C'') and *EphA4*^{-/-} (D-D'') littermates. Myosin in red, b-III tubulin in green. The tibialis anterior, extensor digitorum longus and peroneum longus are innervated in wild-type, but only the peroneum longus is innervated in the mutant. In contrast, the peroneum longus is not innervated in *pma/pma* (Main text, Figure 1). Abbreviations: TA, tibialis anterior; EDL, extensor digitorum longus; PL, peroneus longus. Scale bar represents 50 μm.

Figure S13: Innervation of hindlimbs of P21 mice from EphA4 x pma crosses



Legend: Representative images of gross dissections of sciatic nerve from: (left panel) legs scored as 'normal' with peroneal (P), Tibial (Ti) and Sural (S) branches visible entering the lower limb muscles; (right panel) leg scored as 'absent' with no evidence of a peroneal nerve, though sural and tibial branches remain visible; (middle panel) in absence of a normal peroneal branch, some limbs scored as 'thin' showed evidence of a very thin dorsal nerve which may be a remnant peroneal branch. See Supplementary Table 4 for full dataset.

FIGURE S14 – Jasplakinolide-soaked microsponge on HH stage 20 chicken embryo

